Preparation of Low-Dimensional Cluster Materials: Synthesis, Structure, and Properties of $A_2Ti_2Nb_6Cl_{14}O_5$ (A = K, Rb, Cs), a Series of One-Dimensional Titanium Niobium Oxychlorides

Ekaterina V. Anokhina, Thirumalai Duraisamy, and Abdessadek Lachgar*

Department of Chemistry, Wake Forest University, Winston-Salem, North Carolina 27109

Received May 13, 2002. Revised Manuscript Received July 25, 2002

In the course of our systematic investigation of metal oxychloride systems aimed at the preparation of low-dimensional compounds, a new series of niobium oxychloride cluster compounds, $A_2Ti_2Nb_6Cl_{14}O_5$ (A = K, Rb, Cs), was obtained from stoichiometric amounts of ACl (A = K, Rb, Cs), Ti, Nb_2O_5, $NbCl_5$, and Nb, heated at 750 °C. The crystal structures of the series were determined by single-crystal X-ray diffraction techniques. The compounds crystallize in the monoclinic system, space group *C*2/*c*, with unit cell parameters $a = 21.503(3)$ Å, $b = 8.816(1)$ Å, $c = 15.710(2)$ Å, $\beta = 116.21(1)°$, $V = 2672.1(6)$ Å^3, and $Z = 4$ for A = Rb. The full-matrix least-squares refinement against F^2 converged to R1 = 0.043 ($F_o > 4\sigma(F_o)$) and wR2 = 0.089 (all data for A = Rb). The crystal structure of $A_2Ti_2Nb_6Cl_{14}O_5$ has one-dimensional character. It is based on chains formed by $(Nb_6Cl_7^iO_5^i)Cl_6^a$ octahedral niobium clusters connected to each other through apical chloride ligands and titanium counterions. The chains are held together by alkali metal cations. Intracluster bond distances analysis indicates that the cluster has 14 valence electrons. Magnetic susceptibility study shows paramagnetic behavior with a magnetic moment of 2.17 μ_B per formula unit for two unpaired electrons contributed by two Ti^{3+}.

Introduction

A characteristic feature of compounds containing early transition metals in low oxidation states is the formation of clusters via metal−metal bonding.[1,2] In reduced niobium and tantalum halides and oxides, the most common structural motif is the cluster unit $[(M_6L_{12}^i)L_6^a]^{n-}$ (L = F, Cl, Br, O),[3−5] which consists of an M_6 octahedron surrounded by 12 edge-bridging "inner" (L^i) and 6 apical "outer" (L^a) ligands.[6] In halide compounds obtained through solid-state synthesis techniques, these units can be present as discrete anions or can link to each other by sharing outer and/or inner ligands to form extended structures, the dimensionality of which, with an exception of the structure type of $Na_2Nb_7L_{21}$, is determined by the number of ligands (Table 1).[7−19] In contrast, no direct relationship exists between the composition and cluster connectivity in niobium oxides, which typically have dense three-dimensional frameworks with complex connectivity patterns.[5]

A few years ago we initiated a research program aiming at the preparation of open-framework and low-dimensional cluster materials using a strategy that takes its roots in crystal engineering principles in which desired framework topologies are achieved through the use of building blocks with well-defined directional bonding preferences.[20−22] Our approach is to induce anisotropic bonding preferences in the octahedral cluster

* To whom correspondence should be addressed. E-mail: lachgar@wfu.edu.

(1) Simon, A. *Angew. Chem., Int. Ed. Engl.* **1988**, *27*, 159−183.
(2) Hughbanks, T. *J. Alloys Compd.* **1995,** *229*, 40−53.
(3) Vaughan, P.; Sturdivant, J. H.; Pauling, L. *J. Am. Chem. Soc.* **1950**, 72, 5477.
(4) Perrin, C.; Sergent, M. *Eur. J. Solid State Inorg. Chem.* **1991**, *28*, 933−948.
(5) Köhler, J.; Svensson, G.; Simon, A. *Angew. Chem., Int. Ed. Engl.* **1992**, *31*, 1437−1456.
(6) The notation employed here was initially defined in Schäfer, H.; von Schnering, H. G. *Angew. Chem.* **1964**, *76*, 833−849.
(7) Ihmaïne, S.; Perrin, C.; Peña, O.; Sergent, M. *J. Less-Common Met.* **1988**, *137*, 323−332.
(8) Sitar, J.; Lachgar, A.; Womelsdorf, H.; Meyer, H.-J. *J. Solid State Chem.* **1996**, *122*, 428−431.
(9) Nägele, A.; Anokhina, E.; Sitar, J.; Meyer, H.-J.; Lachgar, A. *Z. Naturforsch. B* **2000**, *55*, 139−144.
(10) Cordier, S.; Hernandez, O.; Perrin, C. *J. Solid State Chem.* **2002**, *163*, 319−324.
(11) Baján, B.; Meyer, H.-J. *Z. Anorg. Allg. Chem.* **1997**, *623*, 791−795.
(12) Baján, B.; Balzer, G.; Meyer, H.-J. *Z. Anorg. Allg. Chem.* **1997**, *623*, 1723−1728.
(13) Womelsdorf, H.; Meyer, H.-J.; Lachgar, A. *Z. Anorg. Allg. Chem.* **1997**, *623*, 908−912.
(14) Cordier, S.; Hernandez, O.; Perrin, C. *J. Solid State Chem.* **2001**, *158*, 327−333.
(15) Cordier, S.; Simon, A. *Solid State Sci.* **1999**, *1*, 199.
(16) Simon, A.; von Schnering, H. G.; Wöhrle, H.; Schäfer, H. *Z. Anorg. Allg. Chem.* **1965**, *339*, 155−170.
(17) Corbett, J. D. In *Modern Perspectives in Inorganic Crystal Chemistry*; Parthé, E., Ed.; Kluwer Academic Publishes: Amsterdam, The Netherlands, 1992.
(18) Tulsky, E. G.; Long, J. R. *Chem. Mater.* **2001**, *13*, 1149−1166.
(19) Perrin, C. *J. Alloys Compd.* **1997**, *262*, 10−21.
(20) Desiraju, G. R. *Angew. Chem., Int. Ed. Engl.* **1995**, *34*, 2311−2327.
(21) (a) Yaghi, O. M.; Li, H. L.; Davis, C.; Richardson, D.; Groy, T. L. *Acc. Chem. Res.* **1998**, *31*, 474−484. (b) Eddaoudi, M.; Moler, D. B.; Li, H.; Chen, B.; Reineke, T. M.; O'Keeffe, M.; Yaghi, O. M. *Acc. Chem. Res.* **2001**, *34*, 319−330.
(22) Aakeroy, C. B. *Acta Crystallogr., Sect. B: Struct. Sci.* **1997**, *53*, 569−586.

10.1021/cm020565p CCC: $22.00
Published on Web 10/02/2002

Table 1. Relationship between the Number of Ligands and Framework Dimensionality in Niobium Halides Containing Octahedral M_6L_{18} Clusters

number of ligands per cluster	dimension	connectivity	structure types	number of phases	examples
18	0D	discrete clusters	5	>40	$KLuNb_6Cl_{18}$[7] $K_2MnNb_6Cl_{18}$[8] $CsTiNb_6Cl_{18}$[9]
17	1D	$(Nb_6L^i_{12})L^{a-a}_{2/2}L^a_4$	1	1	$Cs_2Nb_6Br_5F_{12}$[10]
16	2D	$(Nb_6L^i_{12})L^{a-a}_{4/2}L^a_2$	1	1	$Li_2Nb_6Cl_{16}$[11]
15	3D	$(Nb_6L^i_{12})L^{a-a}_{6/2}$	6	14	$LiNb_6Cl_{15}$[12] $InNb_6Cl_{15}$[13] $Nb_6Br_8F_7$[14] $Na_2(NbF_6)Nb_6Cl_8F_7$[16]
14	3D	$(Nb_6L^i_{10}L^{i-a}_{2/2})L^{a-a}_{4/2}L^{a-i}_{2/2}$	1	1	Nb_6Cl_{14}[15]

Scheme 1. Hypothetical Octahedral Cluster with Four L^{2-} Ligands in the Inner Position[a]

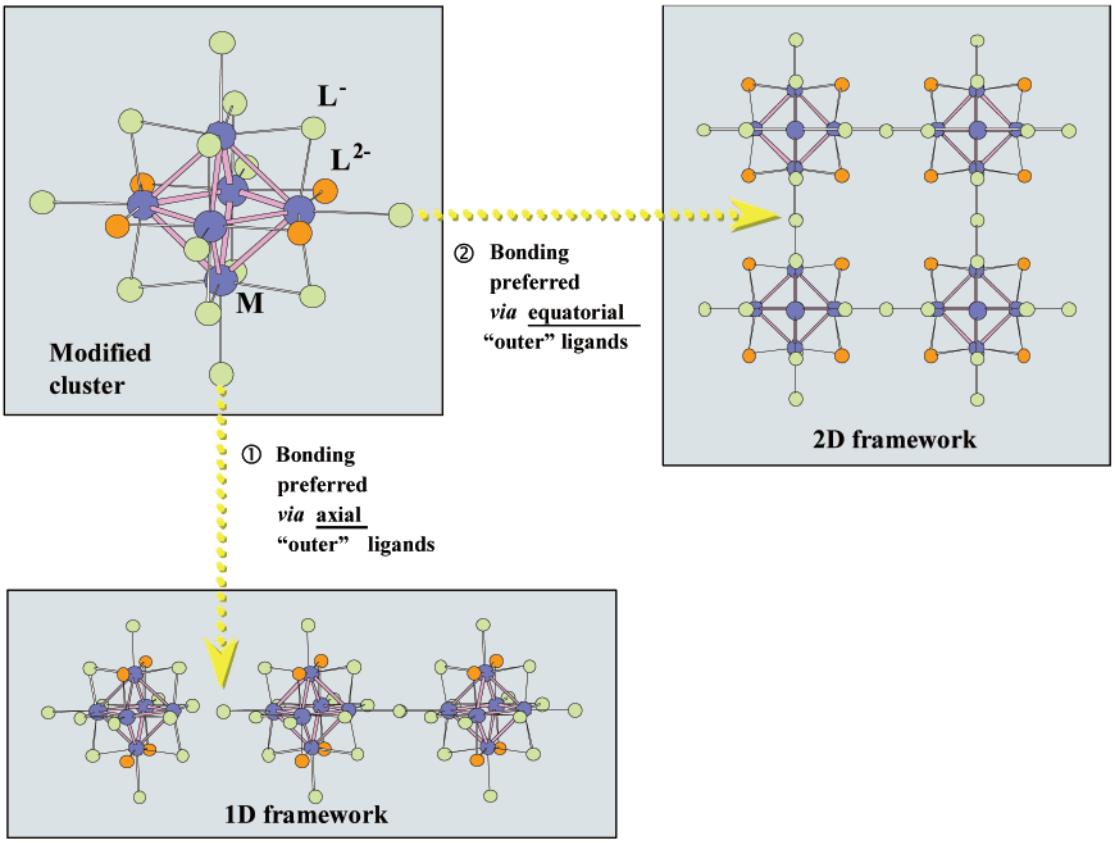

[a] The ligands arrangement can lead to the formation of 1D or 2D cluster frameworks depending on which set of outer ligands (axial or equatorial) is more prone to serve as intercluster bridges.

units by modifying the charge distribution around the metal core using a combination of ligands with a large difference in charge density (Scheme 1). Among several possibilities, we selected the combination of oxide and chloride as ligands in niobium M_6L_{18} clusters because it is one of the rare cases where the following criteria are simultaneously satisfied: *(i) Large difference in ligand charge density*, which decreases the trend of statistical ligand distribution observed in other mixed-ligand systems such as molybdenum and rhenium chalcohalides[23−25] and niobium bromofluorides;[10,14] *(ii)* reduced niobium oxides[5] and chlorides[4,26] that are based on the *same cluster type (M_6L_{18})*, a factor that favors the stabilization of mixed-ligand clusters with a wide range of Cl/O ratios; *(iii) differences between intercluster connectivity trends* (The chlorides are usually characterized by discrete cluster units, while oxides have dense cluster frameworks); and (*iv*) predominance of low-dimensional structures in metals oxychlorides, such as MOCl (M = Fe, Ti, V, Cr, Y, Yb)[27−32] and $MOCl_2$ (M =

(23) Perrin, A.; Perrin, C.; Sergent, M. *J. Less-Common Met.* **1988**, *137*, 241−265.
(24) Perricone, A.; Slougui, A.; Perrin, A. *Solid State Sci.* **1999,** *1*, 657−666.
(25) Mironov, Y. V.; Cody, J. A.; Ibers, J. A. *Acta Crystallogr., Sect. C: Cryst. Struct. Commun.* **1996**, *52*, 281−283.
(26) Perrin, C.; Ihmaïne, S.; Sergent, M. *New J. Chem.* **1988**, *12*, 321−332.
(27) Lind, M. D. *Acta Crystallogr. B: Struct. Sci.* **1970**, *26*, 1058−1062.
(28) Snegireva, E. M.; Troyanov, S. I.; Rybakov, V. B. *Zh. Neorg. Khim.* **1990**, *35*, 1945−1946.
(29) Haase, A.; Brauer, G. *Acta Crystallogr.* **1975**, *31*, 2521−2522.
(30) Forsberg, H. E. *Acta Chem. Scand.* **1962**, *16*, 777−778.
(31) Meyer, G.; Staffel, T. *Z. Anorg. Allg. Chem.* **1986**, *532*, 31−36.

V, Nb, Mo, Ru, Os),[33,34] which are layered, and $NbOCl_3$, which has a 1D framework.[35]

Our investigation of niobium oxychlorides containing titanium as a counterion led to the preparation of two layered materials, $[Tl_5(Ti_2Cl_9)][(Nb_6Cl_{12}O_4)_3(Ti_3Cl_4)_2]$[36] and $Cs_2Ti_3(Nb_6Cl_{12.5}O_4)_2Cl_2$,[37] which have unique hexagonal-bronze-type and graphite-type cluster connectivity, respectively, and $Cs_2Ti_4Nb_6Cl_{18}O_6$,[38] which has a quasi-one-dimensional structure. Prior to our work, Perrin and co-workers were the first to investigate niobium oxychloride systems with the purpose of decreasing intercluster separation and reported the niobium oxychloride cluster compound $ScNb_6Cl_{13}O_3$,[39] which has a acentric three-dimensional framework. Here, we describe the synthesis, crystal structure, and properties of a new series of one-dimensional oxychloride cluster compounds with the idealized composition $A_2Ti_2Nb_6Cl_{14}O_5$ (A = K, Rb, Cs). In this series, the clusters are linked through Cl^{a-a} bridges and $[TiO_2Cl_3]$ square pyramids to form a one-dimensional framework.

Experimental Section

Synthesis. The oxychlorides $K_{1.87(4)}Ti_2Nb_6Cl_{14.23(4)}O_{4.78(4)}$, $Rb_{1.77(3)}Ti_2Nb_6Cl_{14.40(3)}O_{4.60(3)}$, and $Cs_{1.78(2)}Ti_2Nb_6Cl_{14.44(2)}O_{4.56(2)}$ form in high yield (ca. 90%) as long black needles from reactions of Nb powder (Alfa, 99.8%, 325 mesh), Ti foil (Alfa, 99.99%), ACl (Alfa, 99.8%), Nb_2O_5 (Alfa, 99.5%), and $NbCl_5$ (Alfa, 99.9%) in the ratios corresponding to the stoichiometry $A_2Ti_2Nb_6Cl_{14}O_5$ (A = K, Rb, Cs) (eq 1). The mixtures were prepared in an argon atmosphere, sealed in silica tubes (length 4 cm, i.d. 7 mm, o.d. 9 mm) under vacuum, and heated at 750 °C for 4 days, followed by cooling to 500 °C in 36 h and radiative cooling to room temperature. The title compounds

$$8Nb + 12NbCl_5 + 5Nb_2O_5 + 10Ti + 10ACl \xrightarrow{750\ °C;\ \text{sealed silica tube}} 5A_2Ti_2Nb_6Cl_{14}O_5 \quad (1)$$

decompose in air within 2−3 days. They are readily soluble in water, producing intensely colored brown solutions, which is characteristic of niobium halide clusters with 14 valence electrons per cluster.[40] The aqueous solutions become colorless upon exposure to oxygen within several hours.

Elemental Analysis. The reaction products were characterized by semiquantitative energy-dispersive X-ray microanalysis (EDAX). The spectra were obtained with a Philips 515 scanning electron microscope equipped with an EDAX microprobe, at an accelerating voltage of 30 kV, beam diameter of 50−100 μm, and counting times of 50−100 s. The analysis confirmed the presence of alkali metals, Ti, Nb, and Cl.

Phase Analysis. Phase analysis was done by X-ray powder diffraction techniques. Powder patterns were recorded on an automated Phillips diffractometer using Cu Kα radiation. Typical parameters for data collection were as follows: $5° \le 2\theta \le 60°$, step size 0.02°, and counting times 1−3 s. X-ray powder diffraction patterns of the products were consistent with those calculated from single-crystal data and contained weak lines corresponding to Nb_3Cl_8 and $NbOCl_2$.[34,41] The reaction tubes always contained small amounts of colorless liquid droplets, which we attribute to the presence of $TiCl_4$ as a side product.

Crystal Structure Determination. The three phases are isostructural, their crystal habits are the same, and their crystal structure analysis was carried out in a similar manner. Only the structure determination of the rubidium phase is given in detail here. The details on the structural determination of the potassium and cesium phases are submitted as CIF files (see Supporting Information).

A black needle-shaped crystal was selected for X-ray diffraction analysis and mounted in a glass capillary under an argon atmosphere. The intensity data were collected at room temperature on a Bruker P4 diffractometer using Mo Kα radiation. The unit cell parameters were refined based on 40 centered reflections to give a *C*-centered monoclinic unit cell with $a = 21.503(3)$ Å, $b = 8.816(1)$ Å, $c = 15.710(2)$ Å, and $\beta = 116.21(1)°$. The unit cell dimensions and the 2/*m* Laue symmetry were confirmed by axial photographs. The intensity data were corrected for Lorentz and polarization effects, and an analytical absorption correction based on face indexing was applied. The extinction conditions were consistent with the space groups *C*2/*c* and *Cc*. The structure was solved in *C*2/*c* as the intensity statistics indicated a centrosymmetric space group. Initial atomic positions of all atoms except Cl(5)−Cl(8) and O(2) were determined by direct methods.[42]

Subsequently, the remaining atoms were located from Fourier difference maps generated after least-squares refinement cycles.[43] The anisotropic refinement of all atoms with fixed full occupancies yielded R1 = 0.105 and wR2 = 0.207 for all data. The highest residual electron density peak was found to be 4.91 e/Å^3 at 0.76 Å from Rb. The presence of this peak and the large values of thermal parameters of rubidium (U_{11} = 0.255 Å^2, U_{22} = 0.0607 Å^2, and U_{33} = 0.0732 Å^2) indicated splitting of the rubidium position into two closely spaced sites (Rb(1) and Rb(2)). Anisotropic refinement of Rb(1) and Rb(2) positions with released occupancies led to SOF(Rb(1)) = 0.31(1), SOF(Rb(2)) = 0.57(1), and Rb(1)−Rb(2) separation of 0.802(5) Å. The results of these refinement cycles revealed several indications that the Cl(7) inner ligand position is partially occupied by chlorine (when Rb(2) is present) and oxygen (when Rb(1) is present): (i) short Cl(7)−Rb(1) distance of 2.54 Å and longer Cl(7)−Rb(2) distance of 3.33 Å; (ii) short Cl(7)−Nb(2) and Cl(7)−Nb(3) distances (2.345 and 2.369 Å, respectively); (iii) Nb(2)−Nb(3) distance of 2.859 Å, which is longer than the typical distance between oxide-bridged niobium atoms (2.80 Å) and shorter than that for chloride-bridged niobium atoms (2.98 Å); (iv) location of the highest residual electron density peak (1.18 e/Å^3) at 0.93 Å from Cl(7), 1.57 Å from Nb(2), 1.91 Å from Nb(3), and 3.22 Å from Rb(2), which is consistent with the environment of an inner oxide ligand; (v) large thermal parameter value U_{eq}(Cl(7)) = 0.0579(8) Å^2. Isotropic refinement of the L(7) position as being partially occupied by chlorine Cl(7) and oxygen O(7) led to SOF(Cl(7)) = 0.71(3) and SOF(O(7)) = 0.33(6), which is consistent with the occupancies of Rb(2) and Rb(1), respectively. In the subsequent cycles, the Cl(7) and O(7) positions were refined with the restrictions that SOF(O(7)) = SOF(Rb(2)) and SOF(O(7))) + SOF(Cl(7)) = 1. The final refinement cycles converged to R1 = 0.042 and wR2 = 0.076 ($(I > 2\sigma(I))$, R1 = 0.074, and wR2 = 0.086 (all data)), giving the net stoichiometry $Rb_{1.77(3)}Ti_2Nb_6Cl_{14.40(1)}O_{4.60(1)}$, which corresponds to 14.17(6) electrons per cluster. In the following discussion, the composition of the compound has been rounded to $Rb_2Ti_2Nb_6Cl_{14}O_5$ for clarity.

(32) Brandt, G.; Diehl, R. *Mater. Res. Bull.* **1974**, *9*, 411−420.
(33) Seifert, H. J.; Uebach, J. *Z. Anorg. Allg. Chem.* **1981**, *479*, 32−40.
(34) Hillebrecht, H.; Schmidt, P. J.; Rotter, H. W.; Thiele, G.; Zönnchen P.; Bengel, H.; Cantow, H.-J.; Magonov, S. N.; Whangbo M.-H. *J. Alloys Compd.* **1997,** *246*, 70−79.
(35) Sands, D. E.; Zalkin, A.; Elson, R. E. *Acta Crystallogr.* **1959**, *12*, 21−23.
(36) Anokhina, E. V.; Day C. S.; Essig, M. W.; Lachgar, A. *Angew. Chem., Int. Ed. Engl.* **2000**, *39*, 1047−1049.
(37) Anokhina, E. V.; Day C. S.; Lachgar, A. *Chem. Commun.* **2000**, 1491−1492.
(38) Anokhina, E. V.; Day C. S.; Lachgar, A. *Inorg. Chem.* **2001**, *40*, 5072−5076.
(39) Cordier, S.; Perrin, C.; Sergent, M. *Eur. J. Solid State Inorg. Chem.* **1994**, *31*, 1049−1060.
(40) Koknat, F. W.; McCarley, R. E. *Inorg. Chem.* **1972**, *11*, 812−816.
(41) Ströbele, M.; Glaser, J.; Lachgar, A.; Meyer, H.-J. *Z. Anorg. Allg. Chem.* **1997**, *627*, 2002−2004.
(42) Sheldrick, G. M. *SHELXS-97, Program for Structure Solution*; University of Göttingen: Göttingen, Germany.
(43) Sheldrick, G. M. *SHELXL-97, Program for Structure Refinement;* University of Göttingen: Göttingen.

Table 2. Crystal Data and Structure Refinement for $Rb_2Ti_2Nb_6Cl_{14}O_5$

formula	$Rb_{1.77(3)}Ti_2Nb_6Cl_{14.40(1)}O_{4.60(1)}$
formula weight	1387.65
crystal size	$0.75 \times 0.10 \times 0.07$ mm^3
crystal color and habit	black needle
wavelength	Mo Kα (0.71073 Å)
temperature	298 K
crystal system	monoclinic
space group	*C*2/*c* (No. 15)
unit cell dimensions	$a = 21.503(3)$ Å, $b = 8.816(1)$ Å, $c = 15.710(2)$ Å, $\beta = 116.21(1)°$
volume	2672.1(6) Å^3
reflections used for cell determination	40
Z	4
density (calculated)	3.449 g·cm^{-3}
absorption coefficient	7.677 mm^{-1}
F(000)	2547
absorption correction	analytical (face indexing), $T_{min} = 0.45$; $T_{max} = 0.60$
θ range for data collection	2.54° to 29.32°
limiting indices	$-29 \le h \le 1$, $-11 \le k \le 1$, $-19 \le l \le 21$
reflections collected	4090
independent reflections	3365 ($R_{int} = 0.045$)
refinement method	full-matrix least-squares on F^2
data/restraints/parameters	3365/2/147
goodness-of-fit on F^2	1.002[a]
R indices ($I > 2\sigma(I)$)	R1 = 0.042,[b] wR2 = 0.076[c]
R indices (all data)	R1 = 0.0743,[b] wR2 = 0.085[c]
largest diff. peak and hole	0.967 and −0.809 e·Å^{-3}

[a] GOF $= [\Sigma[w(F_o^2 - F_c^2)^2]/(N_{obs} - N_{parameter})]^{1/2}$. [b] R1 $= \Sigma||F_o| - |F_c||/\Sigma|F_o|$. [c] wR2 $= [\Sigma[w(F_o^2 - F_c^2)^2]/\Sigma[w(F_o^2)^2]]^{1/2}$ where $w = 1/[\sigma^2(F_o^2) + (0.0367P)^2]$, $P = (\max(F_o^2, 0) + 2F_c^2)/3$.

Table 3. Summary of Bond Distances (Å) and Angles (deg) in $Rb_2Ti_2Nb_6Cl_{14}O_5$

	(Nb_6L_{18}) Cluster Unit		
$Nb-Nb_{oxide-bridged}$	2.8038(9)−2.8287(8)	Nb−Nb−Nb	57.43(2)−63.43(2)
$Nb-Nb_{chloride-bridged}$	2.9355(9)−2.9901(8)	$Nb-Cl^{a-a}-Nb$	115.68(9)
$Nb-Nb_{Cl(7)-bridged}$	2.8591(9)		
$Nb-Cl^a$	2.605(2)−2.609(2)		
$Nb-Cl^i$	2.368(3)−2.520(2)	$Nb-Cl^i-Nb$	72.43(5)−73.6(1)
$Nb-O^i$	1.92(2)−2.05(2)	$Nb-O^i-Nb$	88.8(2)−92.2(9)
	Ti Environment		
Ti(1)−O	1.923(4)−1.984(4)	L−Ti(1)−L	83.5(1)−158.9(2)
Ti(1)−Cl	2.262(2)−2.480(2)		
	Rb Environment (within 4 Å)		
Rb(1)−O	2.93(2)		
Rb(1)−Cl(6 dist)	3.207(4)−3.661(5)		
Rb(2)−Cl(CN = 9)	3.176(3)−3.991(5)		
	Other Important Distances		
Nb−Ti	3.281(1), 3.350(1)		
Rb(1)−Rb(2)	0.806(4)		
Rb(1)−Cl(7)	2.504(7)		
Cl(7)−O(7)	0.56(2)		

Subsequent refinement of the structure in the noncentrosymmetric space group *Cc* did not lead to new features or lower residuals. Details of data collection and structure refinement are summarized in Table 2, and a summary of important bond lengths is given in Table 3. The details of crystal structure analysis, anisotropic thermal displacements, and the complete listing of bond distances and angles are submitted as Supporting Information.

Magnetic Measurements. The magnetic susceptibility measurements were carried out at 0.5 T in the temperature range 4−300 K on a 26.6-mg microcrystalline sample of $Cs_2Ti_2Nb_6Cl_{14}O_5$ using a Quantum Design MPMS superconducting quantum interference device (SQUID) magnetometer. The crystalline sample was contained in a gelatin capsule fixed inside a plastic straw for immersion into the SQUID. No diamagnetic correction was made for the sample container because its signal was insignificant relative to the sample.

Results

The crystal structure of the new oxychloride series $A_2Ti_2Nb_6Cl_{14}O_5$ is based on a one-dimensional framework formed by octahedral niobium oxychloride clusters linked through outer chlorine ligands (Cl^a) and $[TiCl_3O_2]$ square pyramids. The chains interact with each other through A^+ cations (Figure 1).

The $(Nb_6Cl^i_{7.4}O^i_{4.6})Cl^a_6$ cluster unit consists of a Nb_6 octahedron in which all edges are bridged by chloride or oxide ligands and six other chloride ligands are in apical positions. Four inner ligand positions are fully occupied by oxygen, six by chlorine, and two 70.1(7)% of the time by chlorine (Cl(7)) and 29.9(7)% of the time by oxygen (O(7)) (Figure 2), leading to the formal cluster composition $(Nb_6Cl^i_{7.4}O^i_{4.6})Cl^a_6$. The Nb_6 octahedral cluster core is distorted due to the difference in size and charge of the oxide and chloride ligands. The intracluster bond distances, $Nb-Nb_{(oxide-bridged)} = 2.8038(9)-2.8287(8)$ and $Nb-Nb_{(chloride-bridged)} = 2.9355(9)-2.9901(8)$ Å, are similar to those found in other niobium oxychlorides.[36−39] These bond lengths indicate that the number of valence electrons per cluster core is close to 14,[4,19] as is the case in previously reported oxychlorides with three or more oxygens. Each cluster shares two of

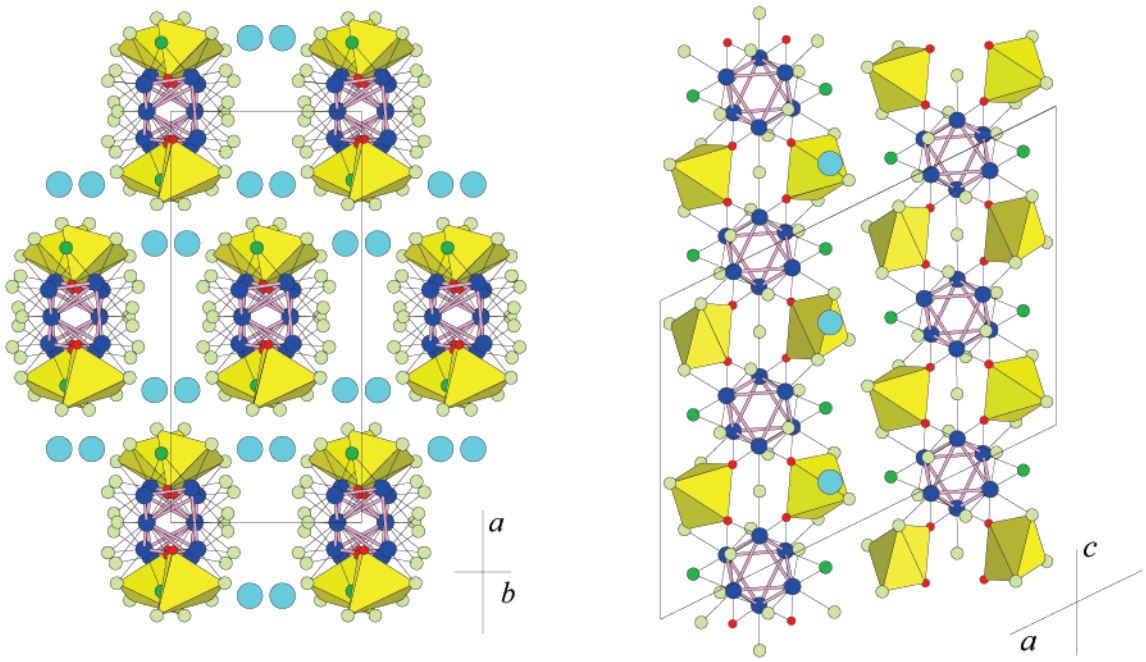

Figure 1. Views of the crystal structure of $Rb_2Ti_2Nb_6Cl_{14}O_5$ in the [001] (left) and [010] (right) directions. Color code: dark blue, niobium; light green, chlorine; red, oxygen; dark green, inner ligand position partially occupied by chlorine and oxygen (Cl(7) and O(7)); light blue, rubidium; yellow, $[TiCl_3O_2]$ square pyramids.

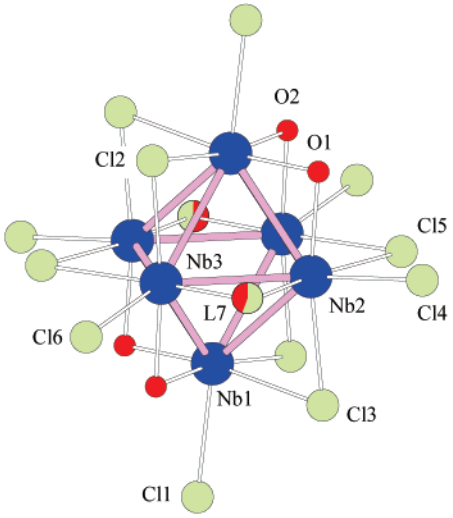

Figure 2. Cluster unit in $Rb_2Ti_2Nb_6Cl_{14}O_5$. Color code: dark blue, niobium; light green, chlorine; red, oxygen; dark green, inner ligand position partially occupied by chlorine and oxygen (Cl(7) and O(7))

its outer chloride ligands with two neighboring units, leading to the formation of zigzag chains (Figure 3) running along the $\vec{c}$ axis with the connectivity formula $(Nb_6L^i_{12})Cl^{a-a}_{2/2}Cl^a_4$. Two titanium atoms per cluster provide additional intercluster linkages within the chain. Each titanium is coordinated by five ligands, two inner oxygens and two outer chlorines (one from each cluster), and one chlorine (Cl(8)) that belongs to titanium only. The two inner oxygens (O(1) and O(2)) and two outer chlorines (Cl(4) and Cl(6)) ligands form the base of a distorted square-pyramidal coordination with $(Ti-O)_{ave.} = 1.953(4)$ and $(Ti-Cl)_{ave.} = 2.448(2)$ Å and are cis with respect to each other. Bond-valence sum calculations[44] indicate that titanium is present in the +3 oxidation state (BVS(Ti) = 3.17).

The chains are held together by rubidium ions that are distributed over two closely spaced, partially occupied positions located between the chains: Rb(1) with the occupancy 29.9(7)% and Rb(2) with the occupancy 58.4(7)%. The Rb(1) position is occupied when the L(7) inner ligand is oxygen, while Rb(2) is present when L(7) is chlorine (Figure 4). Rb(1) coordinates to one oxygen ligand (O(7)) and six chlorines and Rb(2) coordinates to nine chlorines.

Magnetic susceptibility measurements performed on a $Cs_2Ti_2Nb_6Cl_{14}O_5$ powder sample show Curie behavior with an effective magnetic moment of 2.17 μ_B per formula unit (Figure S1 submitted as Supporting Information), which is close to the expected value for two unpaired electrons (2.44 μ_B) from two Ti^{3+} per formula unit. These measurements along with results from bond valence calculations and the dark brown color of an aqueous solution of the phase indicate that the number of valence electrons per cluster is close to 14.

Discussion

To date, the only known examples of one-dimensional compounds containing M_6L_{18}-type octahedral clusters (M = rare earth metals, Zr, Nb, Ta, L = halides) are the zirconium chloride $Ba_2Zr_6Cl_{17}(B)$[45] and the niobium bromofluoride $Cs_2Nb_6Br_5F_{12}$[10] where the clusters form chains via F^{a-a} linkages. In contrast to these structures, the title series, as most other niobium oxychlorides, does not follow the pattern of composition−dimensionality relationship established for compounds containing M_6L_{18} halide clusters (Table 1). Our earlier comparative analysis of the crystal structures of niobium oxychlorides indicated correlations between the cluster frame-

(44) O'Keeffe, M.; Brese, N. E. *J. Am. Chem. Soc.* **1991,** *113,* 3226−3229.
(45) Zhang, J.; Corbett J. D. *J. Less-Common Met.* **1989**, *156*, 49−58.

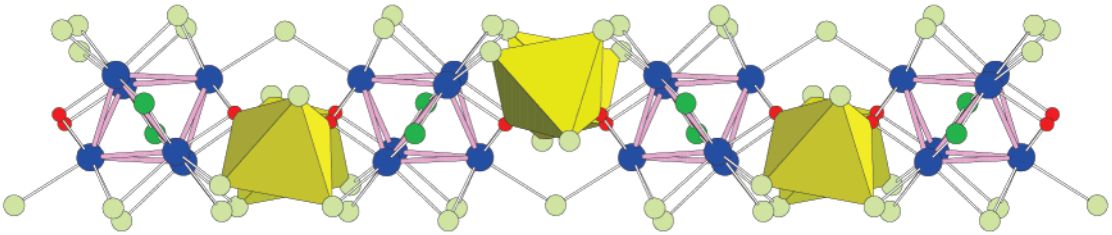

Figure 3. Side view of a chain in $Rb_2Ti_2Nb_6Cl_{14}O_5$. Color code: dark blue, niobium; light green, chlorine; red, oxygen; dark green, inner ligand position partially occupied by chlorine and oxygen (Cl(7) and O(7)); yellow, $[TiCl_3O_2]$ square pyramids.

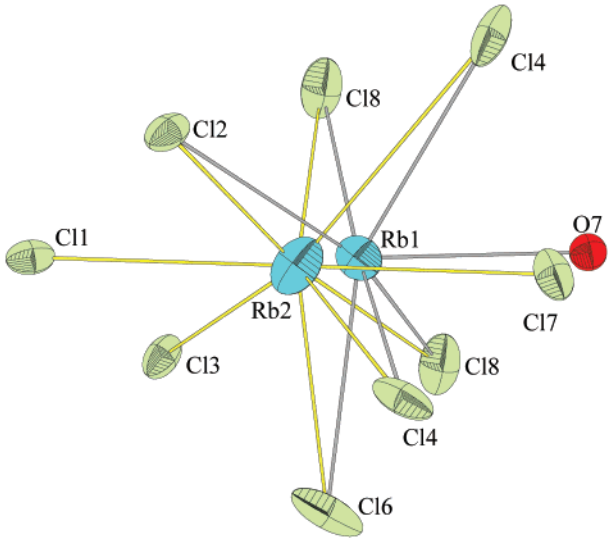

Figure 4. Rubidium environment in $Rb_2Ti_2Nb_6Cl_{14}O_5$. The Rb(1)−L and Rb(2)−Cl bonds are shown in gray and yellow, respectively.

work dimensionality and the ligand arrangement in the cluster unit. In particular, cluster units in which all niobium atoms have equivalent coordination led to compounds containing discrete clusters, while in cluster units where niobium atoms have a different environment, the apical chlorine ligands have different functionalities (bridging and nonbridging), leading to anisotropic cluster frameworks (Table 4). The cluster unit in the title series $A_2Ti_2Nb_6Cl_{14}O_5$ (**I**) (A = K, Rb, Cs) is closely related to the cluster unit $(Nb_6\,Cl^i_8\,O^i_4)Cl^a_6$ found in the compounds $Ti_2Nb_6Cl_{14}O_4$ (**II**)[46] and $[\{Tl_5(Ti_2Cl_9)\}\{Nb_6Cl_{12}O_4\}_3(Ti_3Cl_4)_2]]$ (**III**)[36] in which the four inner oxide ligands have the same arrangement as the four fully occupied oxide ligand positions in **I**. While both cluster units have led to anisotropic cluster networks (one-dimensional in **I** and two-dimensional in **II** and **III**), further investigation is needed to rationalize the change in bonding preferences of the outer chloride ligands, which leads to change in the framework dimensionality upon partial substitution of additional inner chlorides by oxides in **I**.

Another feature that distinguishes the title series from the one-dimensional halides $Ba_2Zr_6Cl_{17}$(B) and $Cs_2Nb_6Br_5F_{12}$ is the bent Nb−Cl^{a-a}−Nb bridges (115.68(9)°) compared to the linear M−L^{a-a}−M bridges in the two latter structures. The bending of the Nb−Cl^{a-a}−Nb bridge is necessary for intercluster linkages via Ti^{3+} counterions to occur (Figure 3). The folding of the cluster chains and the presence of additional chloride ions that do not belong to the clusters (Cl(8)) lead to a more even chain surface compared to an undulated surface in the case of a cluster chain with linear M−L^{a-a}−M bridges. The uneven surface of linear chains leads to stricter steric requirements for an efficient chain packing and results in the change in the packing type upon changing the ligand and/or counterion radii: $Ba_2Zr_6Cl_{17}$(B) has a parallel tetragonal chain stacking, while in $Cs_2Nb_6Br_5F_{12}$, the chains are arranged in layers so that the direction of the chains in a given layer is related to that in the adjacent layer by a rotation of 111.73°. In contrast, the smoother chain surface in the title series allows for the stability of the same parallel hexagonal chain packing type for K, Rb, and Cs. The unit cell parameter change is in agreement with the anisotropic character of the structure: as the counterion radius increases, the *a* and *b* unit cell parameters increase, while *c* (the direction of the chains) remains essentially constant.

Conclusions

The series described here and the previously reported work on niobium oxychloride cluster compounds have demonstrated that a combination of ligands with a large difference in size and charge density leads to anisotropic bonding preferences in the cluster units and favors the formation of low-dimensional cluster materials. A broader and more important implication is the potential of expanding the ligand combination strategy to other transition metal cluster systems. The advances in soft-chemistry techniques open new possibilities for the stabilization of metal and ligand combinations that are not easily accessible by conventional high-temperature techniques, and one can envision that the niobium oxychlorides reported so far represent only a few examples of a large class of mixed-ligand materials with novel structure types yet to be discovered. Recently, Long et al. reported the synthesis of the first tungsten oxychloride octahedral clusters via low-temperature solid-state synthesis followed by cluster excision in solution.[47] This finding confirms the potential for wide

(46) Anokhina, E. V.; Essig, M. W.; Lachgar, A. *Angew. Chem., Int. Ed. Engl.* **1998**, *37*, 522−525.

(47) Crawford, N. R. M.; Long, J. R. *Inorg. Chem.*, **2001**, *40*, 3456−3462.

(48) Cordier, S.; Perrin, C.; Sergent, M. *Mater. Res. Bull.* **1996,** *31*, 683−690.

(49) Cordier, S.; Perrin, C.; Sergent, M. *Mater. Res. Bull.* **1997**, *32*, 25−33.

(50) (a) Anokhina, E. V.; Day, C. S.; Kauzlarich, S. M.; Kim, H.; Lachgar, A.; Meyer, H.-J.; Ströbele, M.; Whangbo, M.-H. *J. Alloys Compd.* **2002**, *338*, 218−228. (b) Gulo, F.; Perrin, C. *J. Mater. Chem.* **2000,** *10*, 1721−1724.

(51) Gulo, F.; Roisnel, T.; Perrin, C. *J. Mater. Chem.* **2001**, *11*, 1237−1241.

Table 4. Summary of Ligand Arrangement and Structural Properties in Reported Niobium Oxychloride Cluster Compounds[a]

1 oxide ligand		**3 oxide ligands**	
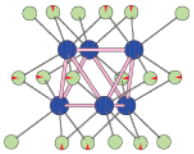		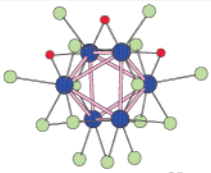	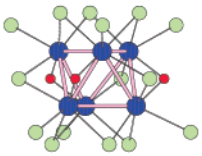
$Cs_2LuNb_6Cl_{17}O$[48]		**$ScNb_6Cl_{13}O_3$**[39]	**$Cs_2UNb_6Cl_{15}O_3$**[49]
CC	**discrete units**	**isotropic 3D**	**discrete units**
OF	**isotropic 3D**	**3D**	**2D**
4 oxide ligands			
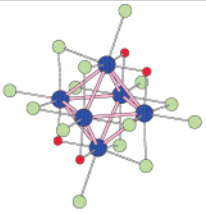		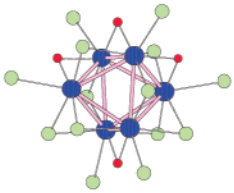	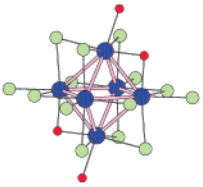
$Ti_2Nb_6Cl_{14}O_4$[46]	**HLF**[b,36]	**$Cs_2Ti_3(Nb_6Cl_{12.5}O_4)_2Cl_2$**[37]	**$MNb_6Cl_{12}O_2$**[50]
CC	**2D**	**2D** HTB	**2D** (graphite topology)	**3D**
OF	**3D**	**2D**	**2D**	**3D**
5 oxide ligands		**6 oxide ligands**	
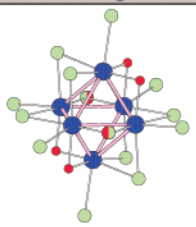		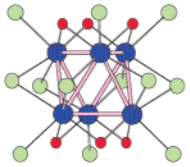	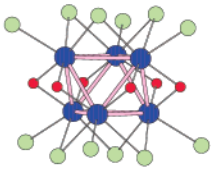
$M_2Ti_2Nb_6Cl_{14}O_5$		**$Cs_2Ti_4Nb_6Cl_{18}O_6$**[38]	**$PbLu_3Nb_6Cl_{15}O_6$**[51]
CC	**1D**	**discrete units**	**discrete units**
OF	**1D**	**quasi 1D**	**isotropic 3D**

[a] The table includes structure types only; related compounds obtained by isomorphic substitution are not listed. Blue spheres, Nb; green spheres, Cl; red spheres, O; green-red spheres, sites partially occupied by Cl and O. Abbreviations: *CC* = cluster connectivity; *OF* = overall framework; HTB = hexagonal tungsten bronze topology. [b] Honeycomb-like layered framework $[Tl_5(Ti_2Cl_9)][(Nb_6Cl_{12}O_4)_3(Ti_3Cl_4)_2]$.

applications of the ligand combination strategy in cluster chemistry.

Acknowledgment. This material is based upon work supported by the National Science Foundation under Grant DMR0070915. Acknowledgment is made to the donors of the Petroleum Research Fund administered by the American Chemical Society, for partial support of this research (ACS-PRF #36080-AC5). We would like to thank Prof. Hans-Conrad zur Loye, University of South Carolina, U.S.A., for magnetic data measurements.

Supporting Information Available: X-ray crystallographic data for the three phases (CIF) and figure showing the inverse molar magnetic susceptibility of $Cs_2Ti_2Nb_6Cl_{14}O_5$ (PDF). This material is available free of charge via the Internet at http://pubs.acs.org.

CM020565P